Università di Pisa

Modeling of ballistic nanoscale metal-oxide-semiconductor field effect transistors

Gianluca Fiori
Dipartimento di Ingegneria dell'Informazione: Elettronica, Informatica, Telecomunicazioni, Università di Pisa
Giuseppe Iannaccone
Dipartimento di Ingegneria dell'Informazione: Elettronica, Informatica, Telecomunicazioni, Università di Pisa

G. Fiori, G. Iannaccone, *Modeling of nanoscale ballistic MOSFETs*, Applied Physics Letters, **81**, pp.3672-3674 (2002).

Modeling of ballistic nanoscale metal-oxide-semiconductor field effect transistors

G. Fiori and G. Iannaccone[a)]
Dipartimento di Ingegneria dell'Informazione, Università degli studi di Pisa, Via Diotisalvi 2, I-56122, Pisa, Italy

(Received 1 July 2002; accepted 13 September 2002)

We present a code for the quantum simulation of ballistic metal-oxide-semiconductor field effect transistors (MOSFETs) in two dimensions, which has been applied to the simulation of a so-called "well-tempered" MOSFET with channel length of 25 nm. Electron confinement at the Si/SiO_2 interface and effective mass anisotropy are properly taken into account. In the assumption of negligible phonon scattering in nanoscale devices, transport is assumed to be purely ballistic. We show that our code can provide the relevant direct-current characteristics of the device by running on a simple high-end personal computer, and can be a useful tool for the extraction of physics-based compact models of nanoscale MOSFETs. © *2002 American Institute of Physics*.
[DOI: 10.1063/1.1519349]

In metal-oxide-semiconductor field effect transistors (MOSFETs) with channel length of a few tens of nanometers expected in the next few years,[1] a significant fraction of electrons contributing to the drain current traverse the channel without undergoing inelastic scattering. The "ballistic" component is expected to increase with further scaling, and to predominate over inelastically scattered electrons in devices with channel length shorter than 30 nm.[2,3]

An analytical model for ballistic MOSFETs has been initially proposed by Natori,[4] and recent simulations based on semiclassical Monte Carlo codes[5] and on a scattering theory of MOSFETs[6] exhibit significant differences with respect to simulations based on drift-diffusion or energy balance models.

Nanoscale MOSFETs also exhibit a significant degree of quantum confinement in the channel due to the high electric field in the direction perpendicular to the Si/SiO_2 interface. A quantum simulation is consequently required to take into account the two-dimensional (2D) subband splitting and the lifting of the sixfold degeneracy of silicon conduction band. This is especially required to reproduce the experimental MOSFET threshold voltage V_T, since semiclassical simulations may underestimate V_T by more than 100 mV.[7]

In this letter we present a code for the two-dimensional simulation of ballistic MOSFETs, in which quantum confinement in the channel is properly taken into account, and electrons are assumed to conserve energy until they reach the drain contact. The code is then applied to the simulation of the so-called "well tempered" MOSFET with channel length of 25 nm proposed by Antoniadis *et al.*[8] as a reasonable candidate for nanoscale MOSFETs and as a benchmark for the validation of simulation codes. To describe the model, let us refer to such a MOSFET structure, whose doping profile is shown in Fig. 1. Source and drain profiles are Gaussian, while super-halo doping is implanted in the channel in order to reduce charge sharing effects. The oxide thickness is 1.5 nm and the channel length is defined by the points where the source and drain doping concentration falls below 2×10^{19} cm^{-3}. The polysilicon gate has donor concentration of 5×10^{20} cm^{-3}.

The Poisson and Schrödinger equations have been solved self-consistently with density functional theory in the two-dimensional domain in strongly confined regions, while a semiclassical approximation has been assumed elsewhere. As we have verified in Ref. 7, the density of states in the longitudinal (y) direction is well approximated by the semiclassical expression, since there is no in-plane confinement, while discretized states appear in the vertical direction, which originate 2D subbands in the channel. Therefore, the one-dimensional Schrödinger equation is solved in the vertical direction (x) for each point of the y axis, with the silicon longitudinal effective mass m_l for the two degenerate conduction band minima along k_x and with the transversal effective mass m_t for the four degenerate conduction band minima along k_y and k_z. Let $E_{il}(y)$ and $E_{it}(y)$ be, respectively, the corresponding eigenvalues ($i=1...\infty$), which also represent the 2D subband edges in the channel. The $I-V$ characteristics have been computed assuming that transport in each subband is fully ballistic. For the purpose of presentation, let us call $E_{SB}(y)$ the generic subband profile and $E_{SB_{max}}=\max_y[E_{SB}(y)]$ [in practice $E_{SB}(y)$ will be substi-

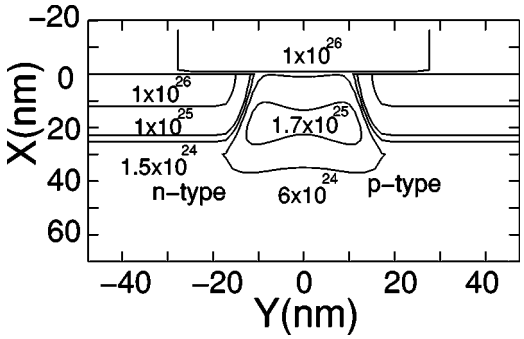

FIG. 1. Contour plots of the doping profile of the 25 nm MOSFET considered in the simulations (concentrations are in m^{-3}).

a)Author to whom correspondence should be addressed; electronic mail: g.iannaccone@iet.unipi.it

tuted by $E_{il}(y)$ or $E_{it}(y)$]. Carriers in the subband with energy larger than $E_{\mathrm{SB}_{max}}$ can be transmitted from source to drain by thermionic emission. Quantum tunneling has not been considered in our model, since it is negligible even in devices with channel length down to 10 nm;[6,9] therefore the transmission coefficient is unity above the maximum of the barrier and zero below. In this way electrons with energy smaller than $E_{\mathrm{SB}_{max}}$ are in thermal equilibrium with the closest contact (source or drain), while electrons with larger energy traverse the channel without energy loss. The electron concentration in the subband is computed by assuming that the states with energy below $E_{\mathrm{SB}_{max}}$ have an occupation factor determined by the Fermi level of the closer reservoir (E_{fS} and E_{fD}, respectively, for source and drain), while states with higher energy propagating from the source to the drain and vice versa have the occupation factor of the originating contact. The total electron concentration is obtained by summing up electron concentrations in each subband over all degenerate conduction band minima. The potential profile is obtained by means of a self-consistent Poisson/Schrödinger solver with a Newton–Raphson method based on a predictor-corrector scheme. Then, the current density per unit length J_{SB} in the subband $E_{\mathrm{SB}}(y)$ can be expressed as a function of $E_{\mathrm{SB}}(y)$, of $E_{\mathrm{SB}_{max}}$ and of the effective mass m_y in the transport direction as follows:

$$J_{\mathrm{SB}}(m_y, E_{\mathrm{SB}}, E_{\mathrm{SB}_{\max}}) = \frac{q}{h^2}\sqrt{2m_y K_B T}\int_{E_{\mathrm{SB}_{\max}}-E_{\mathrm{SB}}}^{+\infty}\left[F_{-1/2}\left(-\frac{E_{\mathrm{SB}}+E_y-E_{fS}}{K_B T}\right) - F_{-1/2}\left(-\frac{E_{\mathrm{SB}}+E_y-E_{fD}}{K_B T}\right)\right]dE_y \quad (1)$$

where $F_{-1/2}$ is the Fermi integral of order $-1/2$. Obviously, J_{SB} is independent of y and therefore Eq. (1) can be computed for an arbitrary value of y in the channel.

Considering all the 2D subbands resulting from mass anisotropy and the six conduction band minima, the total current density per unit length can be written as

$$J = \sum_{i=1}^{\infty}(J_{il} + J_{it}), \quad (2)$$

where J_{il} and J_{it} are the current densities computed for the two degenerate minima in the k_x direction and the four degenerate minima in the k_y and k_z directions, respectively

$$J_{il} = 2J_{\mathrm{SB}}(m_t, E_{il}, E_{il_{\max}}),$$
$$J_{it} = 2J_{\mathrm{SB}}(m_l, E_{it}, E_{it_{\max}}) + 2J_{\mathrm{SB}}(m_t, E_{it}, E_{il_{\max}}), \quad (3)$$

where $E_{il_{\max}}$ and $E_{it_{\max}}$ are the maximum values of $E_{il}(y)$ and $E_{it}(y)$, respectively.

The computed profiles of the first subband for gate voltage $V_{\mathrm{GS}}=1$ V and different values of drain-to-source voltage (V_{DS}) are plotted in Fig. 2. Subband profiles are strongly affected by the overlap of the polysilicon gate with the drain and source regions. The super-halo p doping allows short channel effects to be kept under control:[10,11] as can be seen, the channel barrier is only slightly reduced when the V_{DS} is significantly increased.

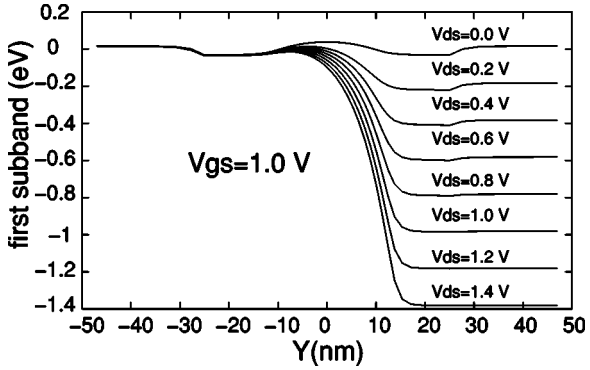

FIG. 2. First subband profile computed for $V_{\mathrm{GS}}=1.0$ V and several values of V_{DS}.

Subband splitting is much larger than the thermal energy, so that practically only the first subband is occupied. Indeed, simulations show that in strong inversion more than 95% of electrons in the channel are in the first subband. The common source output characteristics are shown in Fig. 3. The threshold voltage V_T is close to 0.8 V, depending on the definition used, and is apparently too high for complementary metal-oxide semiconductor circuits with a supply voltage of about 1.5 V. It should be considered that a semiclassical simulation would underestimate the threshold voltage by 170 mV.[7] The output characteristics saturate for small values of V_{DS}, between 0.1 and 0.2 V, since ideal contacts have been considered with zero series resistance.

In Fig. 4 the drain-to-source current (I_{DS}) and the transconductance (g_m) are plotted as a function of V_{GS}. The device exhibits a subthreshold slope close to 100 mV/decade, which is still adequate for obtaining a good $I_{\mathrm{on}}/I_{\mathrm{off}}$ ratio. From the $I_{\mathrm{DS}}(V_{\mathrm{GS}})$ curves for different values of V_{DS}, we can extract a value of the drain induced barrier lowering (DIBL) of 100 mV/V.

In the same figure we also plot, for comparison, the results obtained with the Medici simulator in Ref. 8 with a quantum-corrected drift diffusion model. As can be seen, the subthreshold slope and the DIBL are similar, while an appreciable difference can be observed in the saturation current and in the transconductance. Indeed, in the ballistic regime, a higher current drive is obtained compared to that predicted by a drift-diffusion model.

Figure 5 shows the electron charge density in the channel at a distance from the Si/SiO_2 interface corresponding to

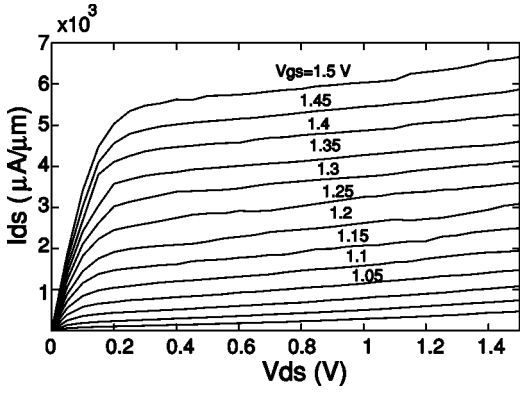

FIG. 3. Common source output characteristics of the 25 nm MOSFET computed with the 2D quantum simulator.

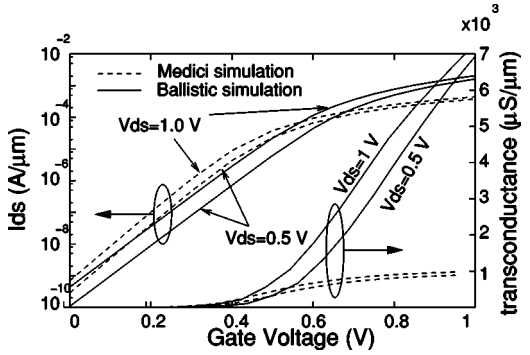

FIG. 4. Current and transconductance vs gate voltage for $V_{DS}=0.5$ V and 1 V obtained with the ballistic model and from MEDICI simulations reported in Ref. 8.

the peak of the electron density (1 nm), the maximum velocity in the channel for electrons with energy equal to the Fermi level of the source, and the average velocity of electrons in the channel. In particular, we can notice that the injection velocity of electrons in the channel is close to the thermal velocity in the longitudinal direction (1.55×10^7 cm/s), in agreement with the fact that in the ballistic regime the thermal velocity is expected to be the upper bound for injection velocity.[12,13]

In conclusion, we have developed a code for the quantum simulation of ballistic MOSFETs in two dimensions and have applied it to the simulation of the so-called well-tempered MOSFETs with channel length of 25 nm. The code runs on a simple high-end PC providing all meaningful dc characteristics and can therefore be a useful tool for device characterization and design.

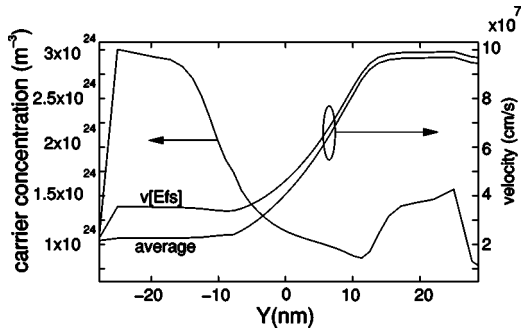

FIG. 5. Electron density, source Fermi level and average velocity in the channel for $V_{GS}=1.2$ V and $V_{DS}=0.5$ V.

Transport in actual devices is not completely ballistic, therefore the model has to be extended in order to take into account those electrons which undergo inelastic scattering.[13] However, the relative importance—and complexity—of such corrections decreases with successive MOSFET generations, as the fraction of ballistic electrons approach unity. This is a great advantage with respect to models based on drift diffusion, in which the zeroth-order assumption is that all carriers thermalize, an then more and more complex corrections must be included, as devices are scaled down, to account for non-equilibrium. The relative simplicity of the proposed transport model allows us to fully include quantum confinement, rather than resort to some correction term. The code has to be thoroughly validated through comparison with data from the electrical characterization of nanoscale MOSFETs. We believe it can represent an important tool for the extraction of physics-based compact models of nanoscale MOSFETs.

Support from the NANOTCAD Project (IST-1999-10828 NANOTCAD) and from Fondazione Cassa di Risparmio di Pisa is gratefully acknowledged.

[1] SIA, *International Technology Roadmap for Semiconductor* (Semiconductor Industry Association, Santa Clara, CA, 2001).
[2] D. J. Frank, S. E. Laux, and M. V. Fischetti, Tech. Dig. - Int. Electron Devices Meet. (IEEE, Piscataway, NJ, 1992), p. 553.
[3] G. Timp, J. Bude, K. K. Bourdelle, J. Garno, A. Ghetti, H. Gossmann, M. Green, G. Forsyth, Y. Kim, R. Kleiman, F. Klemens, A. Kornblit, C. Lochstampfor, W. Mansfield, S. Moccio, T. Sorsch, D. M. Tennant, W. Timp, and R. Tung, Tech. Dig. - Int. Electron Devices Meet. (IEEE, Piscataway, NJ, 1999), p. 55.
[4] K. Natori, J. Appl. Phys. **76**, 4879 (1994).
[5] J. D. Bude, Proceedings of the International Conference on the Simulation of Semiconductor Processes and Devices (SISPAD) 2000 (IEEE, Piscataway, NJ, 2000), p. 23.
[6] M. Lundstrom, Z. Ren, and S. Datta, IEEE Trans. Electron Devices **49**, 133 (2002).
[7] G. Fiori and G. Iannaccone, Nanotechnology **13**, 294 (2002).
[8] D. Antoniadis, I. Djomehri, K. Lackson, and S. Miller, http://www-mtl.mit.edu/Well/(1999).
[9] A. Pirovano, A. Lacaita, and A. S. Spinelli, IEEE Trans. Electron Devices **49**, 25 (2002); J. Appl. Phys. **91**, 2343 (2002).
[10] Y. Taur and T. H. Ning, *Fundamentals of Modern VLSI Devices* (Cambridge University Press, Cambridge, 1998).
[11] Y. Taur, D. A. Buchanan, W. Chen, D. J. Frank, K. E. Ismail, S. H. Lo, G. A. Sail-Lalasz, R. G. Viswanathan, H. J. C. Wann, S. J. Wind, and H. S. Wong, Proc. IEEE **85**, 486 (1997).
[12] Z. Ren, R. Venugopal, S. Datta, and M. Lundstrom, Tech. Dig. - Int. Electron Devices Meet. (IEEE, Piscataway, NJ, 2000), p. 715.
[13] M. Lundstrom, IEEE Electron Device Lett. **18**, 361 (1997).